Electron diffraction study of the structure of vinylidene fluoride–trifluoroethylene copolymer nanocrystals

Mengjun Bai[1,2], X Z Li[2] and Stephen Ducharme[1,2]

[1] Department of Physics and Astronomy, University of Nebraska, Lincoln, NE 68588-0111, USA
[2] Nebraska Center for Materials and Nanoscience, University of Nebraska, Lincoln, NE 68588-0113, USA

E-mail: sducharme1@unl.edu

Abstract
The structures of nanocrystals consisting of 70% vinylidene fluoride and 30% trifluoroethylene made by Langmuir–Blodgett deposition were studied using transmission electron microscopy and electron diffraction. Highly ordered nanocrystals with sizes ranging from 100 nm to 4 μm were grown on Langmuir–Blodgett films at a deposition surface pressure of 20 mN m^{-1}. Electron diffraction patterns from individual crystals allowed us to determine the crystal symmetry and lattice parameters. A monoclinic phase had been found with the lattice parameters $a = 9.06 \pm 0.03$ Å, $b = 5.18 \pm 0.02$ Å, $c = 20.40 \pm 0.05$ Å, $\alpha = 90° \pm 0.3°$, $\beta = 93° \pm 0.2°$, $\gamma = 90° \pm 0.2°$, consistent with the monoclinic space group C_2^3.

1. Introduction

Polyvinylidene fluoride (PVDF) and its copolymers with trifluoroethylene (TrFE) or tetrafluoroethylene (TeFE) are ferroelectric due to spontaneous electrical polarization of the static dipoles [1–3]. For PVDF, several crystal structures have been identified by using x-ray diffraction [4, 5], electron diffraction [6], neutron diffraction [7], and infrared spectroscopy [8, 9]. Previous experimental studies showed that the ferroelectric β phase consists of a planar zigzag all-trans (TTTT) conformation packed two chains per unit cell in an orthorhombic structure with the net dipoles lining up, resulting in a net polarization. Other reported structures contain gauche (G) and anti-gauche ($\bar{\text{G}}$) bonds, including nonpolar α and polar α_p phases with (TGT$\bar{\text{G}}$) conformation [4, 5], a nonpolar randomized variant (TG)$_{0.5}$(T$\bar{\text{G}}$)$_{0.5}$ [7], a polar γ phase with conformation (TTTGTTT$\bar{\text{G}}$) [6], and the helical δ phase with conformation (TGTG) [10, 11]. Molecular modelling [12, 13] studies of PVDF considered nine distinct crystalline structures, including those mentioned above. Random PVDF:TrFE copolymers are found to have some of the same structures as found in PVDF, but with larger lattice parameters in the crystal a–b plane due to the extra fluorine atoms on

the TrFE monomers [2, 7, 9]. Recent studies of ultrathin films of the PVDF:TrFE (70:30) copolymer made by the Langmuir–Blodgett (LB) technique have shown that the copolymer LB films have similar physical properties to the films prepared by other methods such as the Curie point, and polarization reversal [14–17]. In this work, we report the results of structural studies of nanocrystals grown on copolymer LB films, using transmission electron microscopy (TEM) and multi-angle electron diffraction (ED). The ED patterns revealed a structure similar to the most commonly cited orthorhombic structure, but with a 3° monoclinic distortion corresponding to a slight longitudinal displacement between the two chains in the unit cell. Further, the lattice constant along the polymer chain axis $c = 20.4 \pm 0.05$ Å corresponds to eight monomer units, indicating a subtle ordering not previously reported.

2. Experimental details

The copolymer PVDF:TrFE (70:30) films were made by the horizontal (Schaefer) variation of Langmuir–Blodgett (LB) deposition, as described in detail elsewhere [18]. Briefly, this was accomplished by dispersing a 0.01 wt% solution of the polymer in dimethyl sulfoxide on an ultrapure (18 MΩ cm) water subphase, compressing the surface layer of polymer slowly with two barriers, and transferring to the substrate. The surface pressure in this study was 20 mN m^{-1}, much higher than the 5 mN m^{-1} pressure used in the prior studies [18], to promote nanocrystal growth on the film. The substrates were commercial TEM copper mesh grids 3 mm in diameter and coated with a 10 nm thick amorphous carbon film. Electron microscopy and diffraction were performed with a JEOL JEM-2010 transmission electron microscope (200 keV) equipped with double tilt TEM sample holder. A CCD camera (GATAN, DUAL VIEW®) was used to record the images and diffraction patterns. The camera length was calibrated using a similar TEM grid coated with 10 nm of aluminium. The beam current was limited to about 15 pA cm^{-2} to minimize the damage to the sample [19–21].

3. Results and discussions

The LB films transferred at high pressure contained on their surface numerous nanocrystals of various sizes and shapes. One such nanocrystal, shown in figure 1(a), appeared to be a lamellar nanocrystal measuring 510 nm by 420 nm in cross section and of order 60 nm in thickness, as estimated from the beam transmittance. The electron diffraction pattern in figure 1(b) shows that the nanocrystal has a rectangular lattice with quasi-hexagonal symmetry, consistent with the [001] projection along the chains of the copolymer. The diffraction spots were indexed accordingly. Analysis of the diffraction angles for a C-centred unit cell projected on the a–b plane results in lattice parameters $a = 9.06 \pm 0.03$ Å, $b = 5.18 \pm 0.02$ Å and the angle $\gamma = 90° \pm 0.2°$ between the a and b axes. These values are very close to the values $a = 9.05$ Å, $b = 5.12$ Å, $c = 2.55$ Å, $\alpha = \beta = \gamma = 90°$ obtained from powder neutron diffraction studies of the ferroelectric β phase of the 70:30 copolymer and is consistent with the orthorhombic unit cell (space group C_{2v}^{14}) assigned to that structure [7]. The lattice parameters are also small enough to exclude all of the structures containing gauche bonds, since these have a and b spacings about 10% larger than the all-trans β phase, due to the extra space taken up by the gauche bonds [7, 22, 23]. Figure 1(c) shows the lattice image formed from the same crystal under these conditions. Similar quasi-hexagonal electron diffraction patterns for the β phase structure were also reported from PVDF:TrFE (88:12) copolymer single crystals [24] and a PVDF single crystal formed under high pressure, although with different lattice spacings [25]. However, those electron diffraction patterns with the beam along the chain did not give any further information about the period of the chain.
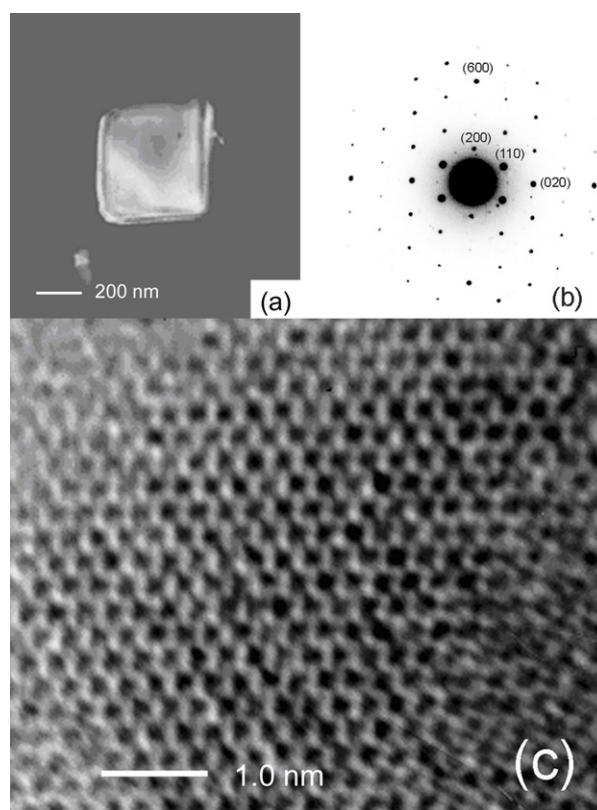
Figure 1. (a) TEM image from a nanocrystal found on an 8-monolayer LB film deposited on a TEM copper grid at a pressure of 5 mN m^{-1} showing the crystalline grains. (b) The ED pattern and (c) the lattice image from the single crystal of image (a). The scale-bar in (c) shows the direction of the *b* axis for the standard β phase lattice.

We also observed that the films contained crystals with other orientations and shapes, such as those shown in figure 2. These differ from the crystal shown in figure 1 mainly by the fact that the crystal chains, which are parallel to the *c* axis indicated by the white arrow, are in the plane of the film. The ED patterns shown in figure 3 from the region indicated by the white circle were recorded at six different angles of incidence by tilting the crystal about the *c* axis. The ED patterns could be indexed according to a monoclinic structure as follows. The pattern in figure 3(a) corresponds to a [010] crystal orientation perpendicular to the a^*–c^* reciprocal lattice plane, and has a fundamental *d*-spacing of 4.52±0.02 Å along (*h*00) and 20.40±0.05 Å along (00*l*) reciprocal lattice vector directions. The angle between the a^* and c^* reciprocal lattice axes is $\beta = 93° \pm 0.2°$, indicating that the unit cell is not orthorhombic, but either monoclinic or triclinic. The pattern shown in figure 3(b), which was obtained by tilting the crystal by 14.2° about the *c* axis, corresponds to a [$\bar{1}$70] crystal orientation, and has *d*-spacings of 1.575 ± 0.02 Å along (710), 10.20 ± 0.03 Å along (00*l*) and 20.40 ± 0.05 Å along (71*l*) directions. Figure 3(c), which was obtained by tilting the crystal by 19.8° about the *c* axis, corresponds to a [$\bar{1}$50] crystal orientation, and has *d*-spacings of 1.708 ± 0.02 Å along (510), 10.20±0.03 Å along (00*l*) and 20.40±0.05 Å along (51*l*) directions. The ED pattern shown in figure 3(d), which was obtained by tilting the crystal by 29.4° about the *c* axis, corresponds to a [$\bar{1}$30] crystal orientation, and has *d*-spacings of 2.607±0.02 Å along (310) and 10.20±0.03 Å
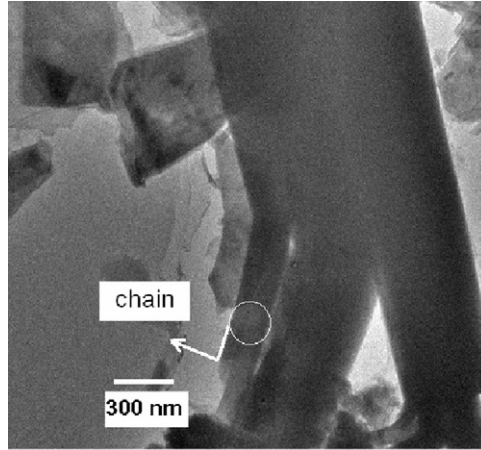
Figure 2. TEM image from a 4-monolayer sample deposited on TEM copper grid at a pressure of 20 mN m^{-1} showing single crystalline grains. The diffraction patterns were recorded from the circled area. The arrow indicates the c axis, identified as the polymer chain direction.

Table 1. The orientations of the selected-area ED patterns shown in figure 3. The tilt angle is the angle from the [010] axis as the sample was tilted about the [001] axis. The calculated tilt angle is obtained from the expression $\tan(\theta) = \frac{a/h}{b/k}$, where $a = 9.06 \pm 0.03$ Å and $b = 5.18 \pm 0.02$ Å.

Image label	(a)	(b)	(c)	(d)	(e)	(f)
Zone axis	[010]	[$\bar{1}$70]	[$\bar{1}$50]	[$\bar{1}$30]	[$\bar{1}$20]	[$\bar{3}$50]
Tilt angle (measured) (deg)	0	14.20	19.80	29.40	41.40	46.48
Tilt angle (calculated) (deg)	0	14.03	19.28	30.24	41.17	46.38

along (00l) and (31l) directions. The missing diffraction spots in figure 3(c) for the (hkl) d-spacings ($l = 2n$, $n = 0, 1, 2 \ldots$, with both h, k even, and $l = 2n+1$, $n = 0, 1, 2 \ldots$ with both h, k odd) are attributed to the identical projections of the potential along or perpendicular to the electron beam direction, respectively. The ED pattern shown in figure 3(e), which was obtained by tilting the crystal by 41.4° about the c axis, corresponds to a [$\bar{1}$20] crystal orientation, and has a d-spacing of 1.704 $\pm$ 0.02 Å along (420) and 10.20 $\pm$ 0.03 Å along (00l) and 20.40 $\pm$ 0.05 Å along (42l) directions. The ED pattern shown in figure 3(f), which was obtained by tilting the crystal by 46.48° about the c axis, corresponds to a [$\bar{3}$50] crystal orientation, and has a d-spacing of 1.56 $\pm$ 0.02 Å along (530), 10.20 $\pm$ 0.03 Å along (00l) and 20.40 $\pm$ 0.05 Å along (53l) directions. The d-spacings from the six selected-area ED patterns shown in figure 3 were recorded for tilt angles ranging from 0° to 46.48° about the c^* axis, as summarized in table 1. A projection of the reciprocal-space lattice onto the a^*–b^* plane, which is perpendicular to the tilting axis (also the chain axis in this case), was constructed from the (hk0) d-spacings from the ED patterns. The diffraction points in the a^*–b^* plane form a quasi-hexagonal periodic pattern (see figure 4) with d-spacings near 4.5 Å for the adjacent spots.

The projection of the real-space lattice onto the a–b plane can be determined by comparing to the standard β phase structure [7] and the structures with trans-gauche bonds, as seen in figure 4. According to the selected unit cell, the a–c plane lattice parameters are $a = 9.06 \pm 0.03$ Å, $c = 20.4 \pm 0.05$ Å, and $\beta = 93° \pm 0.2°$, which can also be obtained directly from figure 3(a). As mentioned above, all known crystal structures of PVDF and PVDF:TrFE copolymers make a quasi-hexagonal packing pattern viewed along the chain, so labelling the
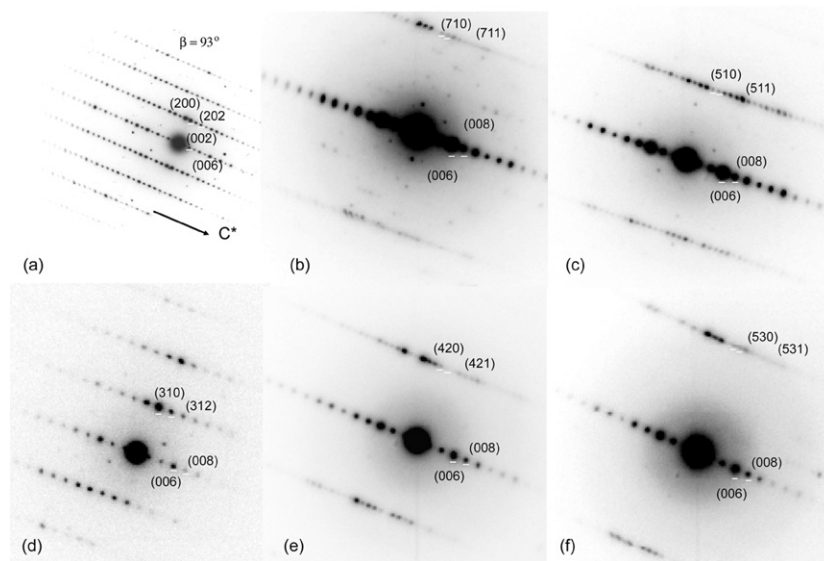
Figure 3. The six ED patterns recorded from the area indicated by the white circle shown in figure 2 by tilting about the *c* axis indicated by the white arrow in figure 2. (a) Along zone [010]. (b) Along zone [$\bar{1}$70]. (c) Along zone [$\bar{1}$50], which is the initial beam direction without tilting. (d) Along zone [$\bar{1}$30]. (e) Along zone [$\bar{1}$20]. (f) Along zone [$\bar{3}$50].
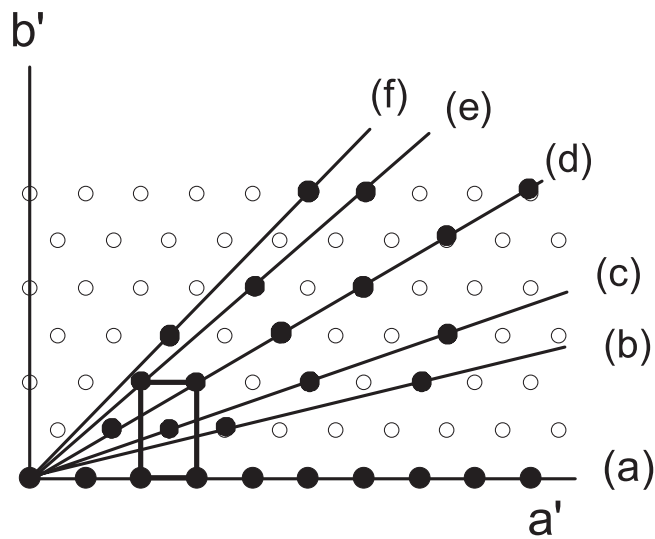
Figure 4. Projection of the reciprocal lattice unit cell onto the *a**–*b** plane, as constructed from the series of ED patterns in figure 3. The solid dots are the experimental data and the circles as well as the lines interpreted from the apparent symmetries are used to guide the eyes. The labelled zone axes indicated the beam direction. The parallelogram shows a reciprocal-space unit cell.

tilting axis to be the *c* (chain) axis is reasonable for this structure because it also has quasi-hexagonal symmetry perpendicular to the *c* axis. The chain orientation is parallel to the film plane with the direction perpendicular to the longer edge of the crystal, as indicated by the arrow in figure 2.

The ED patterns obtained by tilting the crystal contain information useful for constructing the three-dimensional (3D) crystal structure. The patterns along different zone axes can be expressed as a group of numerical equations related to the lattice parameters based on a *more generally triclinic* unit cell with no assumptions about the bond angles or relative lattice spacings. The lattice parameters b, γ (the angle between the a and b axes) and α (the angle between the b and c axes) can be obtained by solving three of the equations with the three known lattice parameters. The results of this analysis give the values $b = 5.18 \pm 0.02$ Å, $\gamma = 89.73° \pm 0.02°$ and $\alpha = 91.6° \pm 1.0°$. Direct measurement from the projection of the 2D unit cell in figure 4 gives $b = 5.18 \pm 0.02$ Å and angles γ and α both close to 90°. Recall that the angle $\gamma = 90° \pm 0.2°$ between the a and c axes has been obtained from the [010] diffraction pattern from figure 1. If we constrain the angle $\gamma = 90°$ we obtain the averaged lattice parameters $b = 5.18 \pm 0.01$ Å, $\alpha = 90° \pm 0.3°$. Unfortunately, the angle α cannot be determined more precisely from the present data due to instrumental limitations. Taken together with the direct measurement of β from figure 3(a), we obtain a monoclinic unit with $\alpha = 90° \pm 0.3°$, $\gamma = 90°$ (fixed), and $\beta = 93° \pm 0.2°$.

So far, the 3D unit cell has been determined based on mapping the unit cell from the ED patterns and calculations of the diffraction equations. All the diffraction patterns in figure 3 can be indexed according to an orthorhombic unit cell. Table 1 lists the experimental tilting angles and the angles calculated according to the lattice parameters with a monoclinic structure, demonstrating good agreement. The maximum angle difference of 0.84° between the experimental and calculated values corresponds to the diffraction pattern with the beam along the [$\bar{1}$30] zone (figure 3(c)), indicating a slight beam tilting away from this direction.

Based on the above analysis, we propose that the structure is similar to the standard β phase, but with monoclinic distortion in the a–c plane and an 8-monomer period along the chain axis. The 20.4 Å repeat period along the chain in this structure, however, is eight times the 2.55 Å length of one monomer unit [7]. There are mechanisms for multiplying the period. According to heuristic and computational models of the all-trans conformation [10, 13], steric hindrance between the fluorines on neighbouring monomers, causes the dihedral angles along the chain to be deflected by about $\pm 6.6°$ from the standard 180° trans bond angle, viewed along the chain direction [13]. In this case, the chain period would be doubled to 5.1 Å. Another possibility is ordering of head-to-head defects or by the TrFE monomers, but the copolymers are generally believed to be random [2, 7, 9]. Previous photoemission studies of the LB films [26] show rectangular symmetry perpendicular to the (110) axis for the copolymer β phase structure, consistent with C_{2v} bulk symmetry.

All diffraction patterns and the projection of the unit cell in the a–b plane showed that it is a C-centred structure in the a–b plane with $(h00)$, $(0k0)$, $(h0l)$, (hkl) satisfying the electron diffraction selection rules: $h = 2n$, $k = 2n$, $h = 2n$, $h + k = 2n$, respectively. For a monoclinic structure, only three *point* groups '**2**', '**m**' and '**m/2**' are possible. If we assume that the distorted β phase is also polar, as discussed above, only two point groups are possible, namely '**2**' and '**m**'. Further, limiting to an all-trans conformation with polarization along the b axis leaves point group '**2**' as the only choice. So the possible crystal symmetry could be determined by combining the point group and the C-centred feature, which is C_2^3 (No. 5), which is different from usual orthorhombic assignment C_{2v}^{14} (No. 38) given for the ferroelectric β phase of PVDF and its copolymers [7, 9]. A similar monoclinic C_2 structure with $\beta = 93°$ and $c = 2.55$ Å was found in VDF copolymers to coexist with either the orthorhombic structure and the hexagonal D_{6h} structure assigned to the paraelectric phase [27, 28]. The monoclinic structure was characterized as a metastable 'cooled' phase in VDF 55% copolymers, where the sequence of phases on heating is monoclinic–orthorhombic–hexagonal [27]. This sequence is consistent with the group–subgroup relationship required for continuous quasi-second-

order phase transitions, where monoclinic C_2 is a subgroup of orthorhombic C_{2v}, which is itself a subgroup of hexagonal D_{6h} [29]. Studies of VDF 60% copolymers suggest that the monoclinic structure also converts directly to the hexagonal structure, which would proceed by a discontinuous first-order transition [28].

4. Conclusions

Electron diffraction patterns from P(VDF–TrFE) 70:30 nanocrystals allowed us to determine the lattice type and parameters. A monoclinic phase had been determined from the electron diffraction patterns by means of two methods: mapping the unit cell and calculations from the diffraction equations; both methods are consistent with each other. The lattice parameters for the all-trans structure obtained from this analysis are $a = 9.06 \pm 0.03$ Å, $b = 5.18 \pm 0.02$ Å, $c = 20.40 \pm 0.05$ Å, $\alpha = 90° \pm 0.3°$, $\beta = 93° \pm 0.2°$, $\gamma = 90° \pm 0.2°$, consistent with a monoclinic space group of C_2^3. Except for the eight-fold period along the c axis, this appears to be the same structure found in other VDF copolymers and variously called the 'cooled' or 'low-temperature disordered' phase. The role of the monoclinic structure in ferroelectric properties, however, is not clear. Perhaps it is only a metastable form, or perhaps a step in a sequence of phase transitions: hexagonal, orthorhombic, monoclinic.

Acknowledgments

References

[1] Lovinger A J 1983 Ferroelectric polymers *Science* **220** 1115–21
[2] Furukawa T 1989 Ferroelectric properties of vinylidene fluoride copolymers *Phase Transit.* **18** 143–211
[3] Nalwa H S (ed) 1995 *Ferroelectric Polymers* (New York: Dekker)
[4] Lando J B, Olf H K and Peterlin A 1966 NMR and x-ray determination of the structure of poly(vinylidene fluoride) *J. Polym. Sci.* A **4** 941
[5] Hasegawa R, Takahashi Y, Chatani Y and Tadokoro H 1972 Crystal structure of three crystalline forms of poly(vinylidene fluoride) *Polym. J.* **3** 600
[6] Lovinger A J 1981 Unit cell of the γ phase of poly(vinylidene fluoride) *Macromolecules* **14** 322–5
[7] Bellet-Amalric E and Legrand J F 1998 Crystalline structures and phase transition of the ferroelectric P(VDF–TrFE) copolymers, a neutron diffraction study *Eur. Phys. J.* B **3** 225–36
[8] Enomoto S, Kawai Y and Sugita M 1968 Infrared spectrum of poly(vinylidene fluoride) *J. Polym. Sci.* A **6** 861–9
[9] Tashiro K 1995 Crystal structure and phase transition of PVDF and related copolymers *Ferroelectric Polymers* ed H S Nalwa (New York: Dekker) pp 63–181
[10] Bachmann M A and Lando J B 1981 A reexamination of the crystal structure of phase ii of poly(vinylidene fluoride) *Macromolecules* **14** 440–6
[11] Davis G T, McKinney J E, Broadhurst M G and Roth S C 1978 Electric-field-induced phase changes in poly(vinylidene fluoride) *J. Appl. Phys.* **49** 4998
[12] Karasawa N and Goddard W A III 1992 Force fields, structures, and properties of poly(vinylidene fluoride) crystals *Macromolecules* **25** 7268–81
[13] Tashiro K, Abe Y and Kobayashi M 1995 Computer simulation of structure and ferroelectric phase transition of vinylidene fluoride copolymers. I. VDF content dependence of the crystal structure *Ferroelectrics* **171** 281–97
[14] Bune A V, Fridkin V M, Ducharme S, Blinov L M, Palto S P, Sorokin A V, Yudin S G and Zlatkin A 1998 Two-dimensional ferroelectric films *Nature* **391** 874–7
[15] Bune A, Ducharme S, Fridkin V M, Blinov L, Palto S, Petukhova N and Yudin S 1995 Novel switching phenomena in ferroelectric Langmuir–Blodgett films *Appl. Phys. Lett.* **67** 3975–7
[16] Ducharme S, Bune A V, Fridkin V M, Blinov L M, Palto S P, Sorokin A V and Yudin S 1998 Critical point in ferroelectric Langmuir–Blodgett polymer films *Phys. Rev.* B **57** 25–8

[17] Blinov L M, Fridkin V M, Palto S P, Bune A V, Dowben P A and Ducharme S 2000 *Usp. Fiz. Nauk* **170** 247–62 (Russian)
Blinov L M, Fridkin V M, Palto S P, Bune A V, Dowben P A and Ducharme S 2000 Two-Dimensional Ferroelectrics *Phys—Usp.* **43** 243–57 (Engl. Transl.)

[18] Ducharme S, Palto S P and Fridkin V M 2002 Ferroelectric polymer Langmuir–Blodgett films *Ferroelectric and Dielectric Thin Films* ed H S Nalwa (San Diego, CA: Academic) pp 545–91

[19] Lovinger A J 1985 Polymorphic transformations in ferroelectric copolymers of vinylidene fluoride induced by electron irradiation *Macromolecules* **18** 910–8

[20] Odajima A, Takase Y, Ishibashi T and Yuasa K 1985 Diffuse phase transition in ferroelectric polymers and its irradiation effect *Japan. J. Appl. Phys. Suppl.* **24** 881

[21] Daudin B, Dubus M and Legrand J F 1987 Effects of electron irradiation and annealing on ferroelectric vinylidene fluoride–trifluoroethylene copolymers *J. Appl. Phys.* **62** 994

[22] Lovinger A J 1982 Poly(vinylidene fluoride) *Developments in Crystalline Polymers* ed D C Basset (London: Applied Sciences) p 195

[23] Bai M 2002 The structure of vinylidene fluoride /trifluoroethylene (PVDF/TrFE) copolymer Langmuir–Blodgett films *PhD Dissertation* University of Nebraska, Lincoln

[24] Koga K, Nakano N, Hattori T and Ohigashi H 1990 Crystallization, field-induced phase transformation, thermally induced phase transition, and piezoelectric activity in P(vinylidene fluoride–TrFE) copolymers with high molar content of vinylidene fluoride *J. Appl. Phys.* **67** 965

[25] Hattori T, Kanaoka M and Ohigashi H 1996 Improved piezoelectricity in thick lamellar beta-form crystals of poly(vinylidene fluoride) crystallized under high pressure *J. Appl. Phys.* **79** 2016

[26] Choi J, Tang S-J, Sprunger P T, Dowben P A, Braun J, Plummer E W, Fridkin V M, Sorokin A V, Palto S P, Petukhova N and Yudin S G 2000 Photoemission band structure symmetries and dipole active modes of crystalline films of vinylidene fluoride (70%) with trifluoroethylene (30%) across the ferroelectric transition(s) *J. Phys.: Condens. Matter* **12** 4735–45

[27] Tashiro K, Takano K and Kobayashi M 1984 Structural study on ferroelectric phase transition of vinylidene fluoride–trifluoroethylene copolymers (III) dependence of transitional behavior on VDF molar content *Ferroelectrics* **57** 297–326

[28] Bellet-Amalric E, Legrand J F, Stock-Schweyer M and Meurer B 1994 Ferroelectric transition under hydrostatic pressure in poly(vinylidene fluoride–trifluoroethylene) copolymers *Polymer* **35** 34–46

[29] Indenbom V L 1960 Phase transitions without change in the number of atoms in the unit cell of the crystal *Sov. Phys.—Crystallogr.* **5** 106–15